Effects of Lignin as a Filler on Properties of Soy Protein Plastics. I. Lignosulfonate

Jin Huang,[1] Lina Zhang,[1] Fangeng Chen[2]

[1]*Department of Chemistry, Wuhan University, Wuhan 430072, People's Republic of China*
[2]*Key Laboratory of Cellulose and Lignocellulosic Chemistry, Chinese Academy of Sciences, Guangzhou 510650, People's Republic of China*

Received 12 April 2002; accepted 27 September 2002

ABSTRACT: A series of biodegradable plastics from soy protein isolate (SPI) and lignosulfonate (LS) with a weight ratio of 0:10 to 6:4 were prepared with 40 wt % glycerol as a plasticizer by compression molding. Their properties were investigated by wide-angle X-ray diffraction (WAXD), differential scanning calorimetry (DSC), dynamical mechanical thermal analysis (DMTA), scanning electron microscopy (SEM), and tensile tests. The results indicated that the introduction of a moderate LS content from 30 to 40 parts in the blends could simultaneously enhance the tensile strength, elongation, and Young's modulus of soy protein plastics alone. Studies of the water sensitivity of the materials suggested that the strong interaction between LS and SPI could restrict the effect of water on the swelling and the damage of the materials, resulting in lower water absorption. The improvement of the properties was attributed mainly to the existence of the beneficial microphase separation and the formation of crosslinked structures because of the introduction of LS into soy protein plastics. Therefore, a model of a crosslinked network formed from SPI molecules with an LS center was established based on the existence of strong physical interactions between LS and SPI. © 2003 Wiley Periodicals, Inc. J Appl Polym Sci 88: 3284–3290, 2003

Key words: glass transition; blends; biodegradable

INTRODUCTION

Petroleum-based plastics improve the life of today's society because of their high strength, lightweight, low cost, easy processibility, and good water-barrier properties. However, these plastics are not biodegradable, resulting in great pollution and litter. There is an increased interest in using renewable, biodegradable, and compostible plastics from starch, cellulose, lignin, protein, and lipid biopolymers for packaging and other industrial applications.[1] Soy protein is an abundant and low-cost protein and, hence, is expectantly being developed into biodegradable plastics due to its renewable, biodegradable, and environmentally friendly features. Soy protein plastics have been prepared by compression molding[2–4] or extrusion[5] methods. In our lab, soy protein plastics were satisfactorily prepared by compression molding, and the effects of the molecular weight from different soy protein fractions and plasticizer content were investigated.[6,7]

Correspondence to: L. Zhang (lnzhang@public.wh.hb.cn).
Contract grant sponsor: National Natural Science Foundation of China; contract grant number: 59933070.
Contract grant sponsors: Hubei Province; Key Laboratory of Cellulose and Lignocellulosic Chemistry, Guangzhou Institute of Chemistry, Chinese Academy of Sciences.

Journal of Applied Polymer Science, Vol. 88, 3284–3290 (2003)

However, these soy protein plastics exhibited a high water absorption and swelling ability. Many chemical and physical modifications were used to enhance the strength, stiffness, and water resistance. The introduction of crosslinking agents, such as formaldehyde, glyoxal, $ZnSO_4$, epichlorohydrin, or glutaraldehyde, could enhance the tensile strength and elongation and lower the water absorption.[5,8] A blend has been widely evaluated as an effective means to improve the properties of polymeric materials for meeting specific needs. Recently, soy protein/modified polyester blend materials were prepared by injection molding. The blends exhibited good miscibility and showed enhanced mechanical strength and reduced moisture sensitivity.[9] In another study, soy protein/polycaprolactone (PCL) blends compatibilized with methylene diphenyl diisocyanate (MDI) were obtained by compression molding.[10] The introduction of PCL enhanced the elongation and toughness, but decreased the tensile strength and Young's modulus. The addition of an MDI compatibilizer to the blend improved the mechanical properties, such as the tensile strength, elongation, toughness, and Young's modulus. In addition, PCL and MDI in the blend effectively restricted the water absorption of the materials. Blends of starch and soy protein have been developed by screw extrusion and injection molding.[11] Cellulose, as a filler, has been blended into soy protein plastics to increase the rigidity of the plastics,[8] and polyphosphate filler has

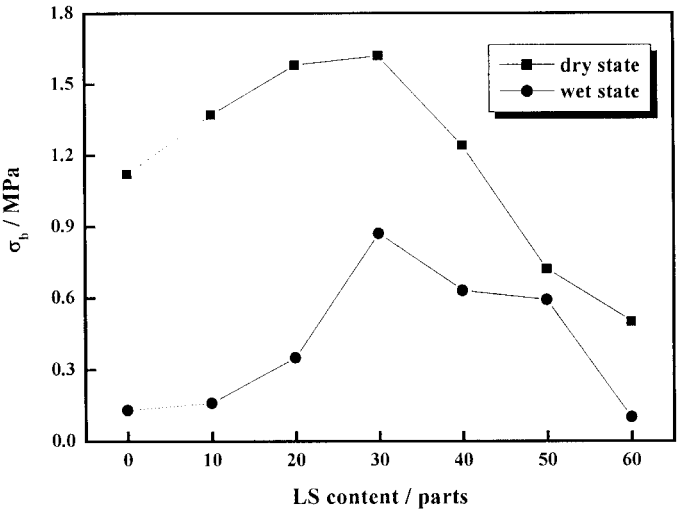

Figure 1 Dependence of tensile strength (σ_b) on LS content of SP–LS sheets in dry and wet states.

also been introduced into soy protein plastics to improve the stiffness, strength, and water resistance.[12]

Lignin is an amorphous natural polymer that is based on phenylpropane derivatives. It has been evaluated as a potential raw material for the chemical industry because it is a nontoxic, commercially available, and low-cost material.[13] Many kinds of industrial lignin, the by-products from pulping and papermaking, have been used as fillers for starch,[14] petroleum-based plastics,[15,16] and rubbers and resins[13] to modify the strength, water resistance, or other properties. In our previous work, 2.8 wt % nitrolignin (NL) was added into a castor oil-based polyurethane elastomer to simultaneously enhance tensile strength and elongation, and a starlike model with an NL center was established.[17] Thus, we attempted to improve the properties of soy protein plastics by adding lignosulfonate (LS) as a filler with many active groups. In this work, the effects of LS on the structure and properties of soy protein plastics were investigated by wide-angle X-ray diffraction, differential scanning calorimetry, dynamical mechanical thermal analysis, scanning electron microscope, and tensile and water absorption tests.

EXPERIMENTAL

Materials and preparation of samples

Soy protein isolate (SPI) with a moisture content of 6.8% was provided by the Yunmeng Protein Technologies Co. (Hubei, China) and used without further treatment. Calcium LS was supplied by the Guangzhou Chemistry Institute of China (Guangzhou, China).

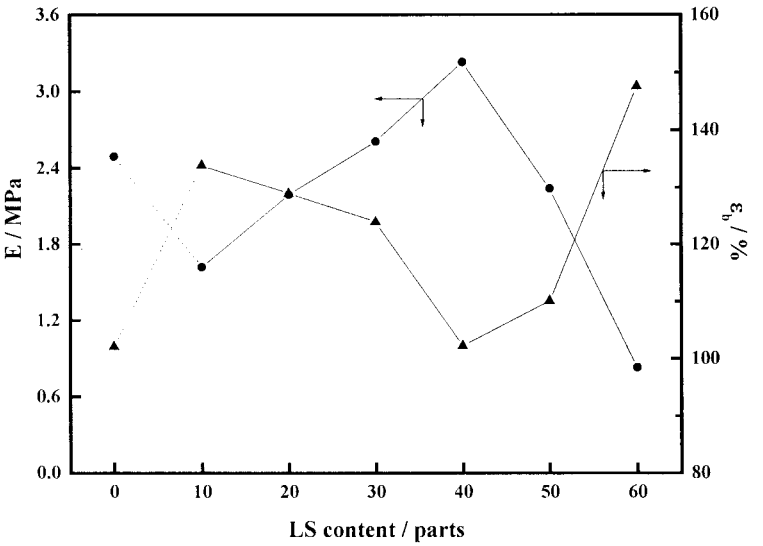

Figure 2 Dependence of elongation at break (ε_b) and Young's modulus (E) on LS content of SP–LS sheets.

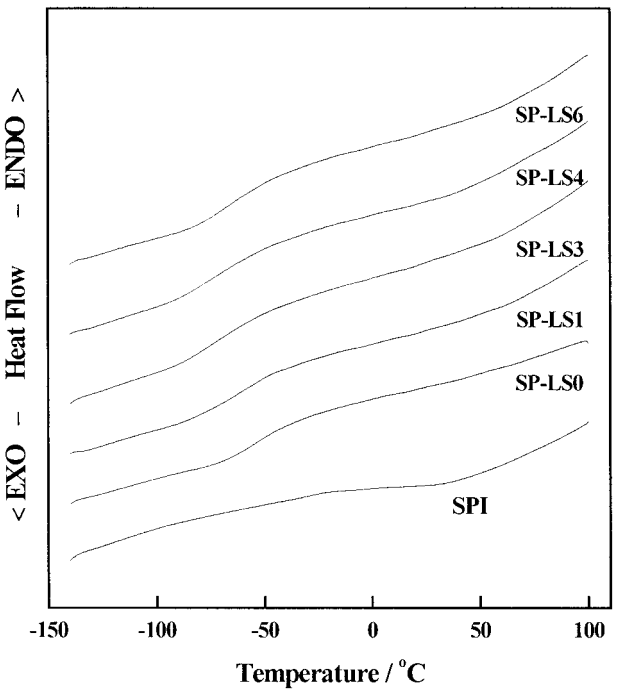

Figure 3 DSC thermograms of SP–LS sheets and SPI.

Analytical-grade glycerol (GL) was purchased from the Shanghai Chemical Co. (Shanghai, China).

Mixtures of SPI and LS (60 wt %, with an SPI of 0, 10, 20, 30, 40, 50, and 60 parts) and 40 wt % GL were mechanically mixed at room temperature, followed by melt blending with an intensive mixer (Brabender Instruments Co., Germany) at 140°C and 30 rpm for 5 min. Subsequently, the blend was placed in a mold covered with two polished stainless-steel plates and then compression-molded using a hot press made by ourselves.[6] The specimen was molded at 160°C and 20 MPa for 3 min and then air-cooled to about 50°C for 0.5 h under constant pressure before removal from the mold to obtain the blend sheets. The sheets were coded as SP–LS0—SP–LS60 according to the LS content from 0 to 60 parts.

Characterization

Wide-angle X-ray diffraction (WAXD) patterns of the sheets were recorded on a D/max-1200 X-ray diffractometer (Rigaku Denki, Japan) with CuKα radiation ($\lambda = 1.5405 \times 10^{-10}$ m), and the samples were examined with 2θ ranging from 6 to 40° at a scanning rate of 10° min^{-1}. Scanning electron microscope (SEM) micrographs were taken on a Hitachi S-570 microscope (Japan). The sheets were frozen in liquid nitrogen and snapped immediately. The cross sections of the sheets were coated with gold for SEM observation.

The tensile strength (σ_b), elongation at break (ε_b), and Young's modulus (E) of the sheets were measured on a CMT6503 universal testing machine (Shenzhen SANS Test Machine Co. Ltd., China) with a tensile rate of 10 mm min^{-1} according to ISO6239-1986 (E). Differential scanning calorimetry (DSC) was performed on a DSC-204 apparatus (Netzsch Co., Germany) under a nitrogen atmosphere at a rate of 10°C min^{-1} from −150 to 100°C. Prior to the test, the samples were heated from room temperature to 100°C to remove moisture and other volatile components in the sheets and then cooled to −150°C at a rate of 20°C min^{-1}.

Dynamic mechanical thermal analysis (DMTA) was carried out using a DMTA-V dynamic mechanical analyzer (Rheometric Scientific Co., USA) at a frequency of 1 Hz. The temperature ranged from −100 to 120°C with a heating rate of 5°C min^{-1}. Thermogravimetric analysis (TGA) curves of the sheets were recorded on a TG 209 thermoanalyzer (Netzsch Co., Germany) under a nitrogen atmosphere from 20 to 800°C at a heating rate of 10°C min^{-1}.

Tests of water sensitivity

Water absorption was measured according to ASTM D570-81 with minor modification. The samples were vacuum-dried for 72 h and then dried at 50°C for 24 h in an oven. Subsequently, they were cooled in a desiccator for a few minutes, weighed, and then submerged in distilled water at room temperature for 2 and 26 h, respectively. The extra water on the surface of the specimen after soaking was removed with a paper towel, and the specimen was weighed again. The container without the soaking specimen was placed in an air oven at 50°C for 72 h to evaporate the water, and the water-soluble content in the specimen was determined. The water absorption (Ab) was calculated according to eq. (1):

$$Ab = (W_1 - W_0 + W_{sol})/W_0 \quad (1)$$

where W_1, W_0, and W_{sol} are the weight of the specimen after water absorption, the weight of the dried specimen, and the weight of water-soluble residuals, respectively.

To study the water resistance (R) of materials, the sheets were immersed in water at the room tempera-

TABLE I
DSC Data and the Degree of Crystalline for the SP–LS Sheets and SPI

Sample	Glass transition		χ_c (%)
	T_g (onset) (°C)	ΔC_p (J g^{-1} K^{-1})	
SPI	—	—	0.31
SP–LS0	−68.4	0.33	0.31
SP–LS10	−81.6	0.35	0.34
SP–LS30	−88.7	0.34	0.37
SP–LS40	−90.4	0.36	0.33
SP–LS60	−81.8	0.40	0.31

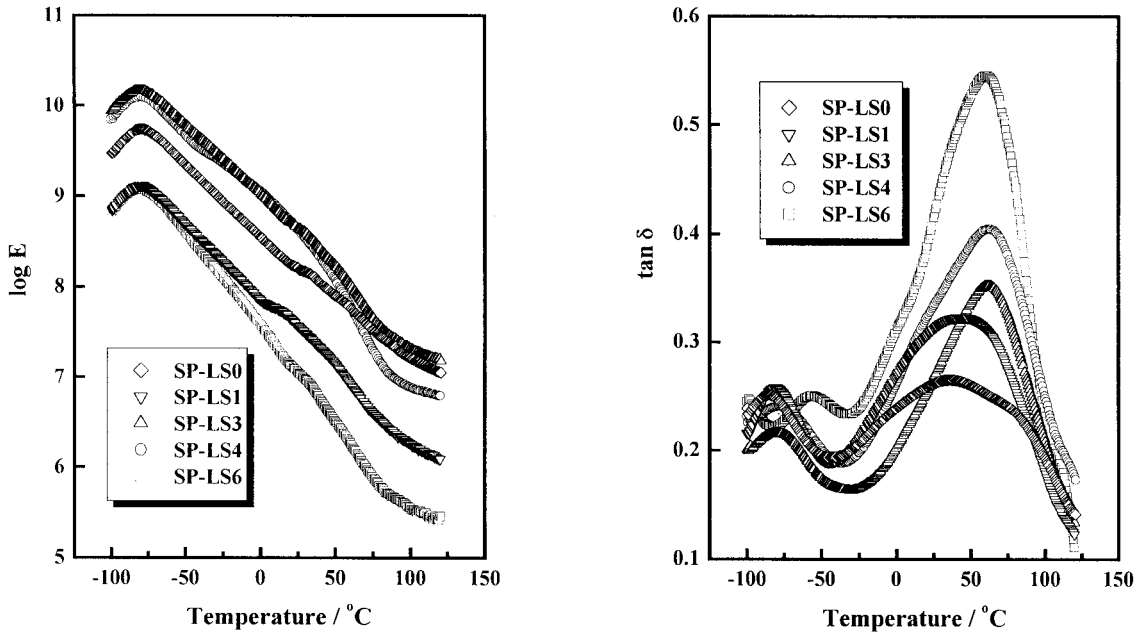

Figure 4 Storage modulus (log E') and tan δ as functions of temperature for the SP–LS sheets.

ture for 1 h. The R values of the sheets were calculated using the following equation:

$$R = \sigma_b(\text{wet})/\sigma_b(\text{dry}) \quad (2)$$

where σ_b(wet) is the tensile strength of the specimen immersed in water for 1 h and σ_b (dry) is the tensile strength of the specimen tested in dry state.[18]

RESULTS AND DISCUSSION

Mechanical properties

The effects of the LS content on the tensile strength (σ_b), elongation at break (ε_b), and Young's modulus (E) for the sheets are shown in Figures 1 and 2. The σ_b of the dry and wet sheets increased with an increase of the LS content up to 30 parts and then decreased, while the σ_b of SP–LS10—SP–LS40 were higher than that of SP–LS0 without LS. The addition of LS can effectively enhance the ε_b of materials, and the ε_b of the sheets containing LS decreased with an increase of LS content up to 40 parts and then sharply increased. The varieties of E values were opposite to those of ε_b, but the E value of SP–LS0 was only lower than that of SP–LS30 and SP–LS40. Interestingly, the LS content ranging from 20 to 30 parts can result in the simultaneous enhancement of σ_b, ε_b, and E for the blends. The stress–strain curves for all the sheets showed that the stress gradually increased with an increase of strain similar to the characteristics of elastomers, and no yield point was observed. Thus, the SP–LS40 with the highest E exhibited a lower σ_b than those of SP–LS20 and SP–LS30 because of its very low ε_b. Similarly, in spite of a higher E for SP–LS0, it worse ε_b resulted in a lower σ_b than those of SP–LS10 and SP–LS20.

The increase of modulus, stiffness, and tensile strength for soy protein plastics can be attributed to strong intra- and intermolecular interactions, such as hydrogen bonding, dipole–dipole, charge–charge, and hydrophobic interactions between polar and nonpolar side chains, which restrict segment rotation and molecular mobility.[3] Calcium LS is a rigid polyelec-

TABLE II
DMTA Data of the SP–LS Sheets

Sample	log E'_{max}	log E'_{25}	α-Relaxation		Loss peak	
			T_α (°C)	tan δ	T_{max} (°C)	tan δ
SP–LS0	9.73	8.23	−85.57	0.252	38.88	0.266
SP–LS10	9.11	7.58	−80.76	0.258	46.05	0.324
SP–LS30	10.18	8.54	−80.51	0.218	61.35	0.354
SP–LS40	10.09	8.60	−78.90	0.242	61.00	0.405
SP–LS60	9.07	7.04	−56.89	0.250	60.73	0.548

Log E'_{max} and log E'_{25} Represented the Maximum log E' Values and log E' at 25°C, respectively.

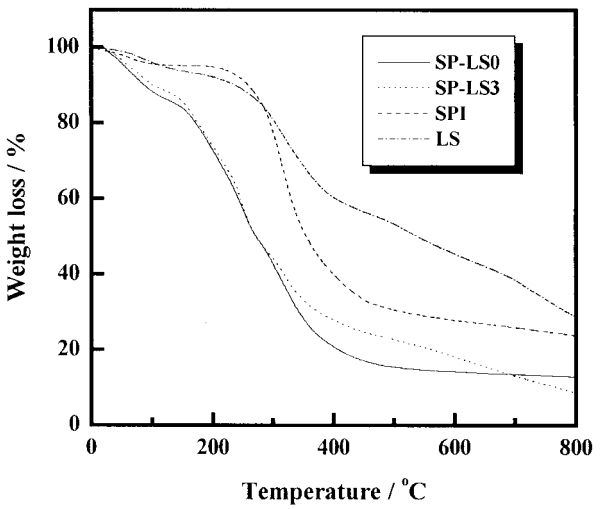

Figure 5 TGA curves of SP–LS sheets, LS, and SPI.

trolyte containing Ca^{2+}, hydrophilic and hydrophobic groups, and many polar groups. Thus, the physical crosslinked network is formed by the strong interactions mentioned above between SPI and LS molecules. When the content of LS is relatively low, it is dispersed into the SPI matrix to become the center of the physical crosslinks, resulting in the enhancement of σ_b and ε_b. As the LS content increases, the LS molecules may be dispersed into the crosslinked network and even restrict the formation of complete networks. Therefore, the LS continuous phase occurred in the SP–LS sheets with an LS content higher than 50 parts, resulting in a decrease of σ_b and an sharp increase of ε_b.

Thermal properties

DSC thermograms of the SP–LS sheets are shown in Figure 3, and the glass transition temperature (T_g) and the change of heat capacities (ΔC_p) are listed in Table I. The combination of the plasticization of GL and the compression process resulted in the obvious glass transition in the range of -91 to -68°C attributed to SPI. The sheets containing LS exhibited a lower T_g than that of SP–LS0, suggesting the existence of microphase separation due to the introduction of LS. The shifts of T_g for the sheets containing LS were correlated to the interaction among GL, LS, and SPI. First, the T_g of the sheets decreased with an increase of LS content and then increased. Both the sheets SP–LS30 and SP–LS40 exhibited a lower T_g, suggesting a change from the SPI continuous phase to the LS continuous phase, and the most obvious microphase separation at 30 and 40 parts LS.

DMTA curves of the SP–LS sheets are shown in Figure 4, and the related data are summarized in Table II. The storage modulus (log E') for the tested sheets first increased with an increase of temperature and then gradually decreased. The values of log E'_{max} and log E'_{25} (log E' at 25°C) for the SP–LS sheets as a function of LS content are similar to those of E measured by the tensile test. The high log E' value at low temperature resulted mainly from the antiplasticization of SPI molecules by GL. The loss modulus (log E'') as function of temperature was the same as that of log E', but two obvious loss peaks appeared in tan δ–T curves for every sheet. The peaks at low temperature of -86 to -56°C were assigned as the α-transition of SPI molecules in the materials. As usual, the T_g from DMTA, considered as T_α, differed from those measured from DSC due to the dynamic nature of DMTA.[19] The tan δ–T curves can usually be utilized to reveal information concerning molecular- and/or segmental-scale motions in polymers, including the effects of molecular interaction and chemical environment. The T_α of the SP–LS sheets increased with an increase of the LS content, suggesting the restriction of LS to SPI molecular motion. This restriction could have resulted from the crosslinked structure and the steric hindrance of the LS phase. In addition, the loss peak at high temperature could result from the thermodynamic relaxation of the materials. Combined with TGA curves shown in Figure 5, the T_{max} of the SP–LS sheets containing LS shifted to a higher temperature up to about 60°C with an increase of the LS content, suggesting that the thermal stability of the materials increased with an increase of the LS content.

Crystalline and morphology

The degree of crystalline (χ_c) and WAXD patterns for SPI and SP–LS sheets with different LS content are

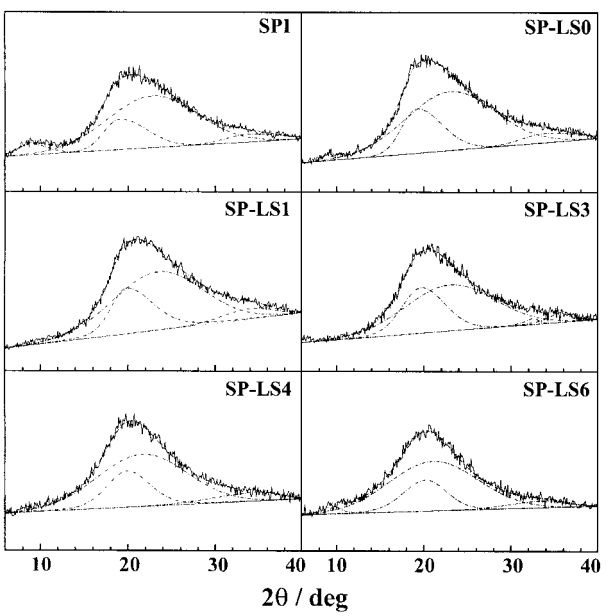

Figure 6 WAXD patterns of SP–LS sheets and SPI. LS was amorphous as proven by WAXD.

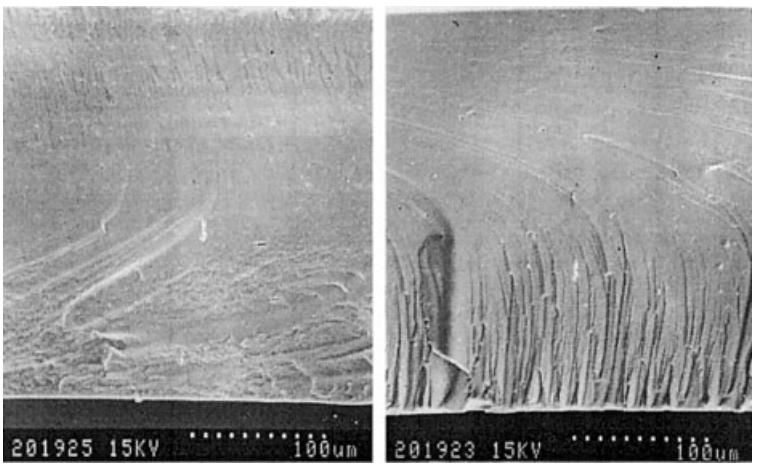

Figure 7 SEM images for SP–LS0 and SP–LS10 sheets.

depicted in Table I and Figure 6, respectively. Usually, the well-miscible blend could result in the decrease of χ_c. However, the sheets containing LS exhibited a higher χ_c than did the sheet without LS (e.g., SP–LS0). It can be explained by that the physical crosslink due to the addition of LS favor the ordered structure of the molecules. The SP–LS30 sheet with the highest σ_b exhibited the maximum value of χ_c, suggesting that the ordered structure is related to higher strength and elongation.

SEC images for the fracture surfaces of SP–LS0 and SP–LS10 sheets are shown in Figure 7. SP–LS0 exhibited a smooth fracture surface. The addition of LS resulted in a coarse and fluctuant fracture surface, displaying some characteristics of tough fracture for the SP–LS10 sheet. This kind of morphology confirmed the enhancement of toughness for the blends.[20]

Water absorption and water resistance

One of the major shortcomings of soy protein plastics are their water sensitivity. As shown in Figures 8 and 9, the introduction of LS efficiently decreased the water absorption (*Ab*) and the swelling extent of the soy protein plastics. The water absorption of the SP–LS sheets decreased with an increase of the LS content up to 40 parts and then slightly increased. At the same time, the water resistance (*R*) of the SP–LS sheets first increased with an increase of the LS content up to 50 parts and then sharply decreased. Since the sulfonic acid group of LS is hydrophilic, the enhancement of resistance to water and reduced swelling could also be attributed to the formation of the crosslinked network. Thus, LS could be utilized to improve the mechanical properties and water resistance of soy protein plastics.

Proposed model for SPI–LS crosslinks

Noting that LS is stiffer than is SPI, the addition of LS could result in the enhancement of σ_b and reduction of ε_b. Interestingly, as shown in Figures 1, 2, and 9, the introduction of LS simultaneously enhanced the strength, toughness, and water resistance of the SP–LS

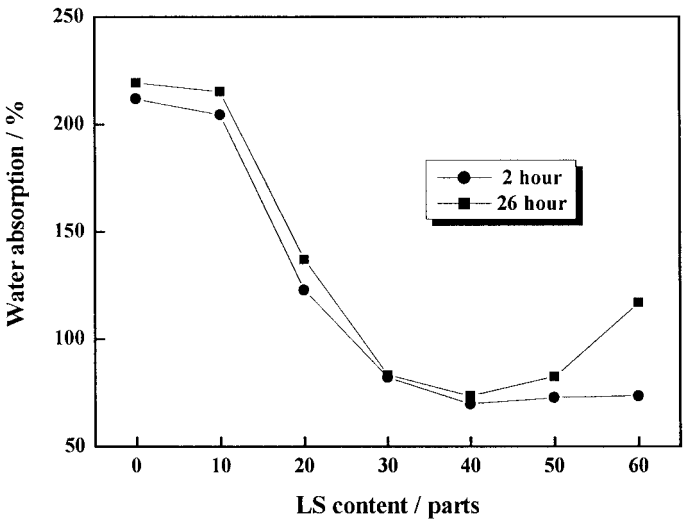

Figure 8 Dependence of water absorption on LS content of SP–LS sheets immersed in water for 2 and 26 h.

blend. Thus, a physical crosslinked structure formed by SPI molecules and an active LS molecule as the center was considered as the most possible structure, resulting in the simultaneous enhancement of σ_b and ε_b. The proposed crosslink structure of the SP–LS sheets with different LS content is depicted in Figure 10. During the heat processing of the blends, the SPI molecules underwent a conformational change from a compact coil to an expanded chain and interacted with the LS center through hydrogen bonding, dipole–dipole, charge–charge, and hydrophobic interactions. When the LS content is moderate, the LS molecules participate to form the complete crosslinked network [Fig. 10(A)]. As the LS contents increase, some LS molecules are dispersed into the crosslinked SPI–LS matrix and slightly restrict the formation of the crosslink [Fig. 10(B)]. When the LS content is higher than 50 parts, the LS molecules form a continuous LS phase, and the crosslinking is further restricted due to the steric hindrance of the LS domain [Fig. 10(C)].

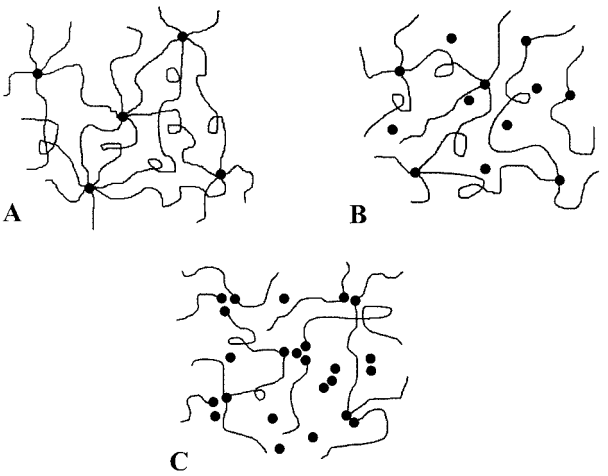

Figure 10 Proposed model of physical crosslinks between (—) SPI and (●) LS molecules in the SP–LS sheets: (A) moderate concentration of LS; (B) high concentration of LS; (C) very high concentration of LS.

CONCLUSIONS

A compositive plastic based on SPI and LS was prepared with glycerol as a plasticizer by the compression-molding method. The SP–LS sheets exhibited higher tensile strength, elongation, and Young's modulus than did the sheet containing SPI alone. It is worth noting that the sheets with a moderate concentration of LS showed enhanced tensile strength and elongation. At the same time, the addition of LS effectively decreased the water absorption of the materials and enhanced the water resistance. The improvement of the properties was attributed mainly to the existence of the beneficial microphase separation and the formation of a physical crosslinked network between SPI and LS. Therefore, a physical crosslinked structure between with SPI molecules and active LS molecule as the center was proposed as the most possible structure.

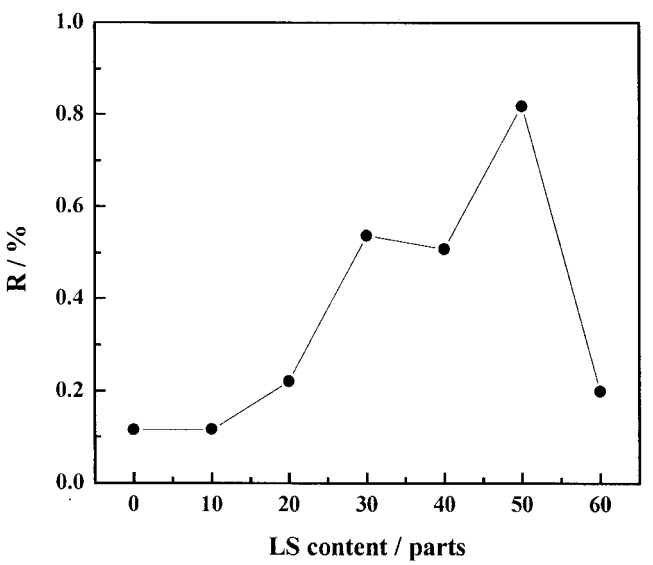

Figure 9 Dependence of water resistance (R) on LS content of SP–LS sheets immersed in water for 1 h.

This work was supported by a Major Grant of the National Natural Science Foundation of China (59933070), a Major Grant of Science and Technology Project from Hubei Province, and the Key Laboratory of Cellulose and Lignocellulosic Chemistry, Guangzhou Institute of Chemistry, Chinese Academy of Sciences.

References

1. Chandra, R.; Rustgi, R. Prog Polym Sci 1998, 23, 1273.
2. Paetau, I.; Chen, C.; Jane, J. Ind Eng Chem Res 1994, 33, 1821.
3. Sue, H. J.; Wang, S.; Jane, J. Polymer 1997, 38, 5035.
4. Mo, X.; Sun, X. S.; Wang, Y. J Appl Polym Sci 1999, 73, 2595.
5. Zhang, J.; Mungara, P.; Jane, J. Polymer 2001, 42, 2569.
6. Wu, Q.; Zhang, L. Ind Eng Chem Res 2001, 40, 1879.
7. Wu, Q.; Zhang, L. J Appl Polym Sci 2001, 82. 3373.
8. Paetau, I.; Chen, C. Z.; Jane, J. J Environ Polym Degrad 1994, 2, 211.
9. John, J.; Bhattacharya, M. Polym Int 1999, 48, 1165.
10. Zhong, Z.; Sun, X. S. Polymer 2001, 42, 6961.
11. Huang, H. C.; Chang, T. C.; Jane, J. JAOCS 1999, 76, 1101.
12. Otaigbe, J. U.; Adams, D. O. J Environ Polym Degrad 1997, 5, 199.
13. Wang, J.; Manley, R.; Feldman, D. Prog Polym Sci 1992, 17, 611.
14. Baumberger, S.; Lapierre, C.; Monties, B.; Valle, G. D. Polym Degrad Stab 1998, 99, 273.
15. Alexy, P.; Kosikova, B.; Podstranska, G. Polymer 2000, 41, 4901.
16. Levon, K.; Huhtala, J.; Malm, B.; Lindberg, J. J. Polymer 1987, 28, 745.
17. Huang, J.; Zhang, L. Polymer 2002, 43, 2287.
18. Zhang, L.; Liu, H.; Yan, S.; Yang, G. J Polym Sci Part B Polym Phys 1997, 35, 2495.
19. Gao, S.; Zhang, L. Macromolecules 2001, 34, 2202.
20. Zhong, Z. K.; Sun, X. S. J Appl Polym Sci 2001, 81, 16.